Available online at www.sciencedirect.com
ScienceDirect
Physics Procedia 1 (2008) 51–60
Physics Procedia
www.elsevier.com/locate/procedia

Proceedings of the Seventh International Conference on Charged Particle Optics

Electrospray ionisation source incorporating electrodynamic ion focusing and conveying

Alex W. Colburn*, M. P. Barrow, M. C. Gill, A. E. Giannakopulos, Peter J. Derrick

Institute of Mass Spectrometry and Department of Chemistry, University of Warwick, Coventry CV4 7AL, United Kingdom

Received 9 July 2008; received in revised form 9 July 2008; accepted 9 July 2008

Abstract

The control and transmission of charged entities in the intermediate to high pressure regime is of primary importance in areas such as atmospheric pressure ionisation. In an electrospray ionisation source where small apertures separate differentially pumped vacuum regions in the inlet systems to mass spectrometers, a large proportion of the available ion current is lost to the surrounding electrode structures. A new electrospray ionisation source, incorporating electrodynamic focusing and conveying of charged entities in two vacuum regions is described. The new source design incorporates ion accumulation and pulsed extraction to allow application in techniques such as Fourier Transform Ion Cyclotron Resonance and orthogonal time-of-flight where a pulsed ion source in required. The design of the new source is described and preliminary experimental results using an orthogonal time-of-flight configuration are presented.

PACS: 07.77.Ka; 41.85.-p; 07.75.+h

Keywords: Electrospray ionisation source; Electrodynamic ion focusing; Mass spectrometer

1. Introduction

The introduction of electrospray ionisation (ESI) by Fenn and coworkers [1-3] has provided a powerful tool for the analysis of biological macromolecules. Electrospray ionisation (ESI) is an ionisation method which operates at atmospheric pressure. Fig. 1 shows a schematic diagram of a typical ESI source configuration. A solution of analyte molecules is sprayed from the tip of a needle held at high potential producing a very fine aerosol of charged droplets. The motion of the droplets is dominated by the bulk transfer properties of the surrounding gas that carry the droplets towards and through an aperture (often a capillary tube) into the first vacuum region of the ion source where the pressure is usually between 1mbar and 10mbar. A second aperture (often a conical skimmer) allows a portion of the expanding jet from the first aperture to pass into the high vacuum region ($<10^{-6}$ mbar) of the mass spectrometer [4]. The apertures form conductance restrictions between each vacuum stage necessary for the differential pumping system to operate efficiently. During the passage from atmospheric pressure to the high

* Corresponding author. Tel.: +44-2476-523-192
E-mail address: a.w.colburn@warwick.ac.uk.

doi:10.1016/j.phpro.2008.07.077

vacuum within a mass spectrometer, evaporation of the solvent in the droplet occurs finally resulting in the production of molecule ions [5].

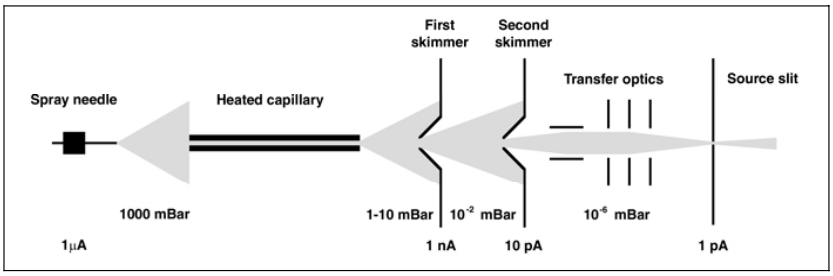

Fig. 1. Schematic diagram of a typical ESI source configuration

Many current designs of ESI source exhibit poor transmission efficiency due to the considerable loss of charged entities to parts surrounding the apertures. Experimental measurements [6] have shown that it is not unusual for less than 1 part in 10^3 of the available current to pass through the first aperture and for less than 1 part in 10^2 of that to pass through the second aperture. Overall, less than 1 part in 10^5 of the electrospray needle current may be available as ion current into the mass spectrometer. In order to improve transmission efficiency, a mechanism of focusing the charged entities into the apertures is required. Conventional electrostatic optics does not work efficaciously in the higher-pressure regions due to the large number of collisions with surrounding gas molecules. Electrostatic optics typically requires the energy of transmitted entities to be conserved during their passage through the optical system.

Gerlich [7] has extensively discussed the focusing and transmission of ions using electrodynamic techniques. Kirchner *et al* [8] have employed Paul trapping to control ions in a large electrode array ion processing unit. The Kirchner design has found a commercial application in the form of the "T-Wave" based instruments available from Waters Instruments. More recently, Smith *et al* have reported an "ion funnel" device [9,10] operating in the intermediate pressure region (0.1 – 10mbar). The device consisted of a series of cylindrical ring electrodes with progressively smaller internal diameter. Operation of the ion funnel required the co-application of radio frequency (RF) and static (DC) fields. The RF field provided collisional focusing of ions radially in the same manner as the Paul trap [11], generating a series of static ion traps along the axis of the device. Combination of the RF and DC fields distorted the ion traps in the direction along the central axis of the device promoting easier transfer of ions between adjacent traps. The motive force for transmission of ions through the device was repulsive space charge effects as ions built up in the traps. Smith *et al* reported [10] an order of magnitude increase in ion current and ion signal compared to those from a conventional ESI ion source. The device was limited by a RF amplitude-related m/z transmission window. Smith *et al* identified [10] the pseudo-potential well depth of the traps (particularly at the base of the ion funnel) as the principle cause of the limited m/z transmission window and as the principle limit on transmission. To reduce the pseudo-potential well depth the thickness and spacing of the electrodes was reduced to provide an increased aperture to spacing ratio. Smith *et al* reported [13] a 2 – 5 fold increase in the ion current transmission over the previous design and a significant improvement in low-mass transmission (m/z > 200). Subsequent incorporation of the ion funnel design in the ESI source of a FTICR mass spectrometer led to a report of zeptomolar sensitivity [13].

2. Ion conveyor principle of operation

This group has reported a new electrodynamic ion focusing and conveying device, the ion conveyor [14]. The electrodynamic device described here produces a fluctuating electric field that has the property of radially focusing, trapping and transmitting charged entities entering the device. This device is related to the ion funnel but the method of controlling the charged entities is significantly different. The mechanism of operation is the application of multiple voltage waveforms to a repetitive series of ring electrodes where the relative phase and shape of the

waveforms is tailored to produce the desired fluctuating electric field. Fig. 2 shows an example of a series of suitable voltage waveforms, which we call conveyor waveforms. In this case, these are four sinusoids phase-shifted 90° with respect to each other. Fig. 3 shows the electrode structure to which the voltage waveforms would be applied, consisting of a series of square parallel plates with a circular aperture. Other cross-sections such as elliptical or rectangular may be envisaged, such shapes being used to define the symmetric or asymmetric performance of the device. The conveyor waveforms are applied to the electrodes sequentially and repetitively according to the number of phases employed.

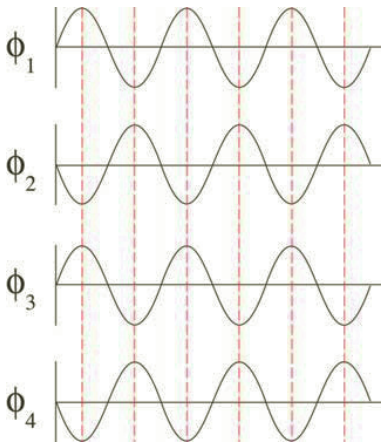

Fig. 2. An example of a series of conveyor waveforms, in this case four sinusoids phaseshifted 90° with respect to each other.

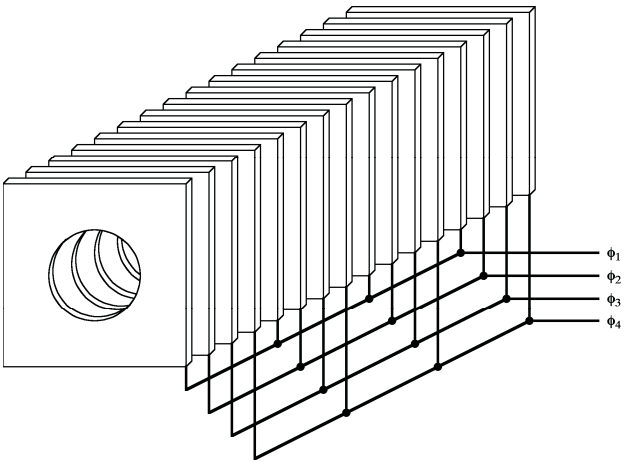

Fig. 3. An example of an electrode structure to which the voltage waveforms would be applied.

The effect of the conveyor waveforms is to produce a travelling wave as a function of time, which is reproduced in the electric field produced within the electrode structure. Reversal in the order of the conveyor waveforms causes the wave to propagate in the opposite direction. This four-phase sinusoid configuration is the lowest-order solution providing a smooth propagation wave. Equation 1 shows the relationship between the propagation velocity of the wave (v), electrode spacing (l) and frequency of applied conveyor waveforms (f).

$$v = 4lf \tag{1}$$

The action of this travelling wave is to convey any charged entity within the electric field in the direction of propagation of the wave, providing motive force for transmission through the device. The radial focusing action of this device is due to the time division in ion residence of positive and negative regions of the field.

3. Simulations

Ion trajectory simulations have been performed using SIMION 3D version 7.0 [15]. in conjunction with a user program developed “in house”. All trajectory calculations were carried out using a three-dimensional electrode array of size 21 x 21 x 121 grid points using a scale factor of 1 mm per grid point. The user program was written to simulate the alternating potentials applied to the electrodes and the effect of collisions between the simulated ions and a hypothetical background gas. To simulate the alternating electric field, the user program varied the applied potentials in discrete steps at a much higher frequency (>10) than the alternating potential. Each step employed the SIMION 7.0 fast-adjust technique, which makes use of the additive solution property of the Laplace equation, to refine a new potential array. The user program simulated the effects of collisions by introducing a mean free path between collisions and a kinetic energy loss per collision. Different pressure regimes were simulated by varying the

mean free path of the ion between collisions. The percentage kinetic energy loss during a collision was determined randomly according to a normal distribution, falling between zero and a user-defined upper limit. Trajectory simulations were carried out using a range of singly-charged ions of mass up to 10 kDaltons. Using the operating conditions described in the following results it was found that all ions in the mass range 200 to 5 kDaltons were focused and transmitted through the device. The initial position and starting conditions of the ions was varied over a range of initial energies up to 10 keV and angles to the optical axis up to 45º. The very large energy and angular acceptance results are a consequence of the very large number of collisions that occur during motion through the device.

Fig. 4 shows a 2-dimensional plot of ion trajectory simulations utilising the waveforms shown in Fig. 2 applied to the electrode structure shown in Fig. 3. Three trajectories for an ion of mass 1 kDalton with initial energy 200 eV are shown from a series of starting positions across the entrance aperture to the device. The mean-free-path and energy loss per collision parameters were set to simulate a medium range pressure of approximately 4 mbar. Collisional damping caused the ions to rapidly lose kinetic energy and prompt radial focussing of the ions towards the central axis of the device occurs. Motion of the ions is characterised by propagation along the device with a superimposed orbiting motion which collapses into an oscillatory motion in the direction of propagation as the ions approach the central axis. The oscillatory motion is caused by the combination of propagating electric field and collisional damping. If a stationary ion is considered at the centre of the device, the leading edge of the propagating electric field wave will accelerate the ion according to its mass-to-charge ratio and current position in relation to the leading edge. Collisions resulting from the acceleration and consequent kinetic energy loss cause the ion to slip backwards in phase with respect to the propagating wave causing the ion to experience the deceleration and eventual directional change produced by the trailing edge of the wave. The repetition of this acceleration and deceleration cycle is manifested as oscillatory motion.

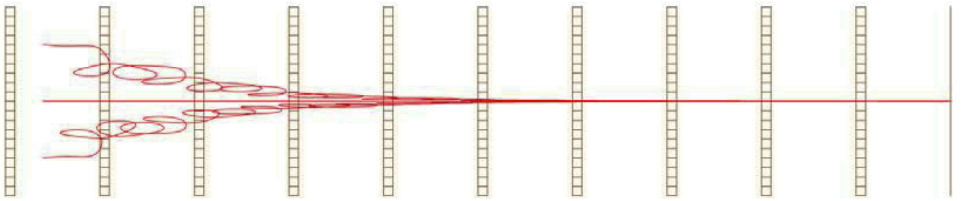

Fig. 4. A 2-dimensional plot of ion trajectories simulated at higher intermediate pressures.

At pressures below 1 mbar where the mean free path is large and the kinetic energy loss due to collisions is small the efficiency of radial focusing decreases. This is because the velocity of the ion carries it away from a particular region well before it has experienced the influence of a full cycle of the alternating electric field. Radial focusing may be restored at lower pressures by modifying the waveform of the applied alternating voltages. If anti-phase RF voltages of much higher frequency than the conveyor waveforms are applied to alternate electrodes a series of static Paul traps is generated along the axis of the device providing efficient radial focusing in low pressure regions. Fig. 5 shows an example of a series of waveforms to provide Paul trapping in the ring electrode stack. To transmit the radially focused ions through the device the conveyor waveforms are electronically summed with the anti-phase RF voltages to produce “composite” waveforms. The effect of the waveform summation is to generate a travelling electrostatic ripple along the axis of the electrode structure which promotes transmission between Paul traps in the direction of propagation. Fig. 6 shows a 2-dimensional plot of ion trajectory simulations where the “composite” waveforms are applied to the electrode stack. It can be seen from Fig. 6 that by application of the “composite” waveforms the radial focusing and transmission properties of the device can be restored to a similar level to those demonstrated at higher pressures.

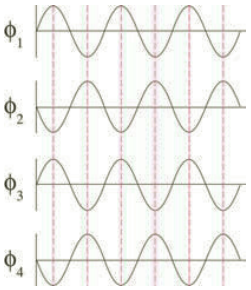

Fig. 5. An example of a series of waveforms to provide Paul trapping in the ring electrode stack.

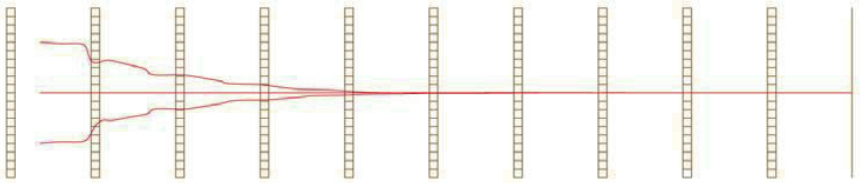

Fig. 6. A 2-dimensional plot of ion trajectories from the results of ion trajectory simulations utilising the "composite" waveforms in low pressure regions.

4. Source Design

Electrospray ionisation sources designed to operate with mass analysers such as Fourier Transform Ion Cyclotron Resonance (FTICR) or orthogonal time-of-flight (TOF) are functionally different to those designed for use on continuous beam analysers. The pulsed nature of FTICR and TOF analysers dictates that the ion source itself should be pulsed to make efficient use of the ion current available. Since electrospray ionisation is intrinsically a continuous process an ion accumulation device such as a multipole storage device is usually inserted between the source and analyser. Ions are accumulated in the storage device and extracted as a dense ion packet as required by the duty cycle of the mass analyser.

Fig. 7 shows a schematic diagram of the new source design. The analyte solution is sprayed from an off-axis needle assembly mounted a few mm from the atmospheric pressure end of a glass capillary and held at ground potential. The needle assembly is equipped with a nebulising gas sheath and position adjustable in three dimensions. The commercially available (Analytic Inc., Branford, USA) glass capillary was 180 mm long, 6.5 mm outside diameter, 0.4 mm internal diameter with 30 mm of metallization at each end. Electrospray current is generated by applying a -4 kV to -5 kV potential to the atmospheric pressure end of the capillary. A counter flow of nitrogen gas heated to 150 ºC is used to promote desolvation of the electrospray droplets. The vacuum end of the capillary is pumped by an 18 m^3/hr rotary pump through a variable conductance restriction to facilitate pressure control in this region and is held at a potential between 0 V and 200 V. The bulk flow properties of gas drawn into the capillary entrain the charged droplets allowing them to be lifted through the potential gradient applied across the ends of the capillary. A ring electrode stack consisting of 33 electrode plates was positioned 3 mm from the end of the glass capillary. Each electrode was 10 mm in diameter with a 3.2 mm central hole and manufactured from 0.2 mm thick 316S16 stainless steel by precision chemical etching. The electrode stack was supported on a 1.27 mm spacing and the necessary electrical connections made using printed circuit boards (PCB's). Four-phase conveyor waveforms were applied to 32 of the electrodes and a variable DC potential was applied to the first entry electrode. The second vacuum region of the source was pumped by a 250 ls^{-1} turbomolecular pump with a variable conductance restriction mounted in front of the pump to control pressure in this region. A 3 mm thick plate with 1 mm central hole and electrically isolated from the source body separated the first and second vacuum regions and acted as the exit electrode for the first stage electrode stack and a conductance restriction between the two vacuum stages. A second ring electrode stack with the same geometry as the first electrode stack but consisting of 44 electrode plates was positioned 1.5 mm from the plate separating the vacuum stages. A second 3 mm thick plate with 1 mm central hole was mounted 1.5 mm from the end of the second electrode stack and acted as a conductance restriction between the second stage vacuum region and the high vacuum of the mass spectrometer. Fig. 8 shows the axial DC potential profile of the ion source in accumulation and extraction modes. In accumulation mode, DC offsets were applied to the electrode stacks and entry/exit electrodes to form a potential well within the second stage electrode stack. The continuous beam of ions transmitted by the first stage ion conveyor is accumulated in the second stage conveyor by a combination of the axial potential well and the radial trapping resulting from the application of RF potentials to the electrode stack. In extraction mode, the trap/extract electrode potential was taken

to 0 V allowing ions to exit the second ion conveyor with a mean kinetic energy determined by the DC offset applied to the electrode stack. To enable efficient clearing of ions accumulated in the second conveyor, composite waveforms were applied to the second conveyor whenever the trap/extract electrode potential was taken to 0 V.

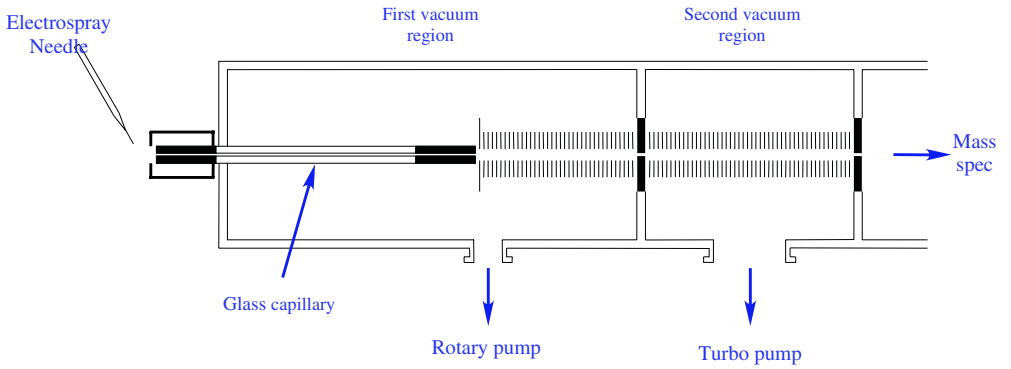

Fig. 7. A schematic diagram of the new source design.

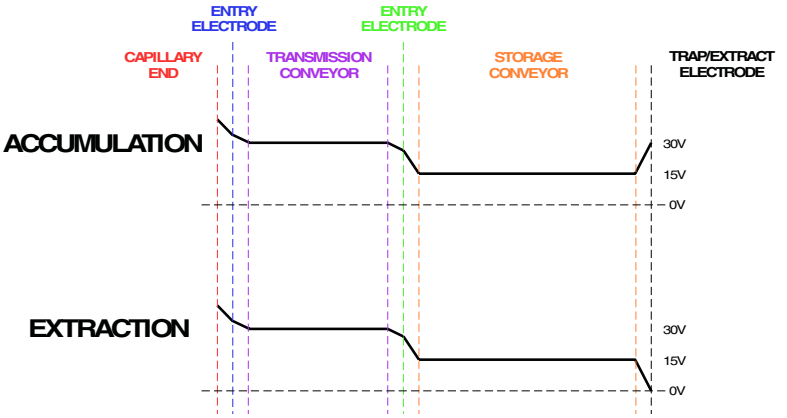

Fig. 8. Axial DC potential profile of ion source in accumulation and extraction modes.

Fig. 9 shows a schematic diagram of the electronic system designed in house to operate the ion conveyor. The four phase conveyor waveforms were generated using a four channel digital frequency generator. Each phase was amplified and DC offset using an LM3886 (National Instruments) audio power amplifier before application to a summing transformer. An RF signal generator (Thurlby Thandar Instruments model TG550) was set to produce the desired frequency for the trapping waveforms and amplified with a broadband 50W RF power amplifier (Amplifier Research model KMA1040M14) before application to the summing transformers which were driven in a series/parallel bridge mode. Each summing transformer was custom wound on Ferroxcube ETD29 ferrite cores and impedance matched for the frequency being employed. DC potentials for entry and exit electrodes were derived from regulated bipolar power supplies via a precision 10-turn potentiometer.

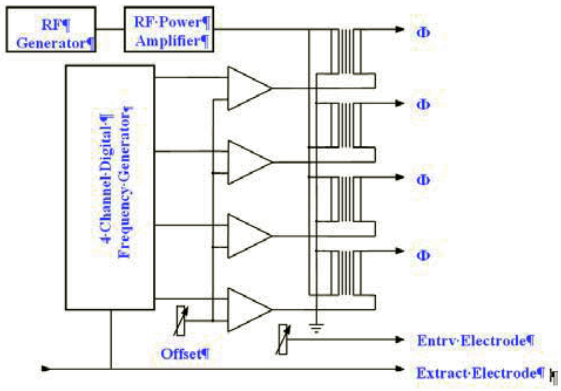

Fig. 9. Schematic diagram of the electronic system designed to operate the ion conveyor.

5. Experimental results

Preliminary experimental results were obtained with the electrospray source fitted to a Bruker Daltonics (Billerica, USA) orthogonal time-of-flight (TOF) instrument operated in reflectron mode. To measure the transmission characteristics of the first stage ion conveyor the electrodes of the second stage conveyor were directly connected to an electrometer (Keithley Instruments model 602) and the proportion of ion current striking the electrodes was recorded as a function of pressure in the second vacuum stage. Fig. 10 shows a plot of total ion transmission for bovine insulin in the first stage ion conveyor as a function of pressure over a range of waveform frequencies. The measured transmission window extended over an order of magnitude in pressure from 3 mbar to 25 mbar with peak transmission observed at approximately 12.5 mbar. Transmission curves for waveform frequencies ranging from 10.31 kHz to 50 kHz were recorded and showed essentially similar characteristics with some variation in overall magnitude in current. Fig. 11 shows a series of mass spectra of bovine insulin over a range of pressures in the first stage vacuum region. The overall intensity of peaks in the mass spectra follow a similar trend to that observed in the transmission curves shown in Fig. 10 and the relative intensity of peaks remains substantially constant indicating the m/z transmission window does not change significantly over the operating pressure range.

Fig. 12 shows the mass spectrum of bovine insulin (mol. wt. 5733.49) obtained using the ion conveyor source. The concentration of the analyte solution was 90μM in a 1:1 water/acetonitrile solvent with 1% acetic acid added. The first stage ion conveyor was operated with conveyor waveforms set to 20.7 kHz and 32 V p-p amplitude at a pressure of 12 mbar. The second stage ion conveyor was operated with trapping waveforms set to 450 kHz and 20 V p-p at a pressure of 4 x 10^{-2} mbar. The mass spectrum is characteristic of ESI spectra for this analyte with the three dominant peaks representing the 3+, 4+ and 5+ charge states.

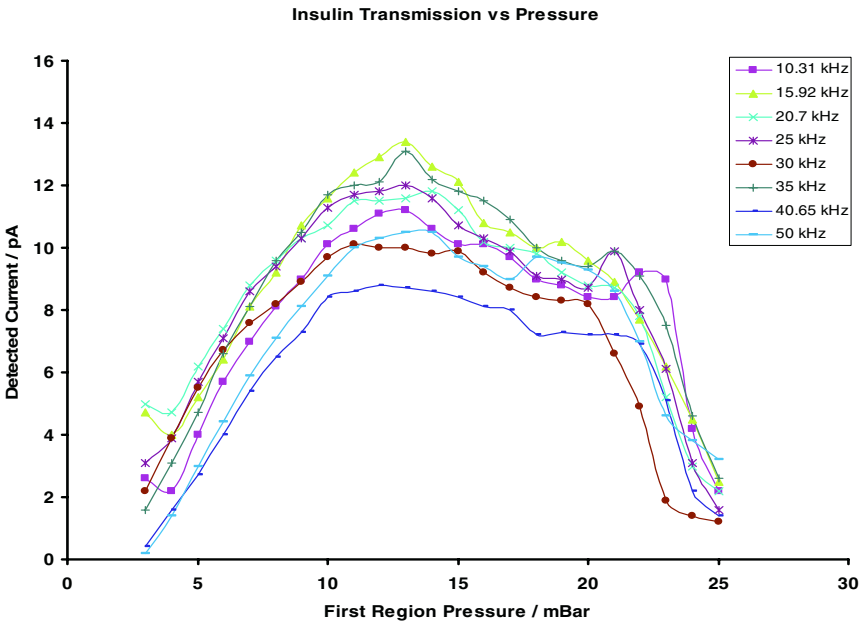

Fig. 10. Bovine insulin total ion transmission for the first stage ion conveyor as a function of pressure and waveform frequency.

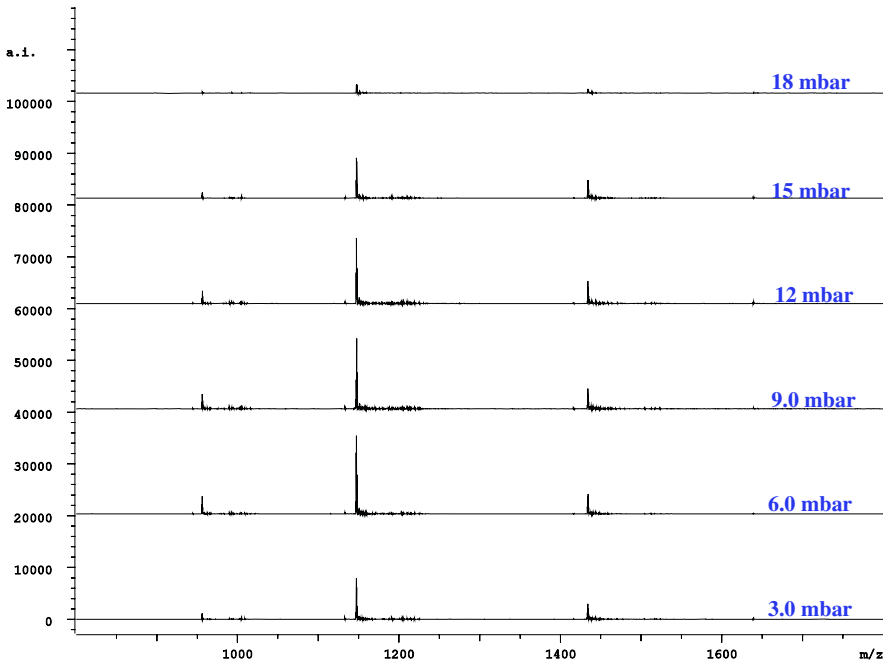

Fig. 11. Electrospray ionisation mass spectra of bovine insulin for a range of pressures in the first stage vacuum region.

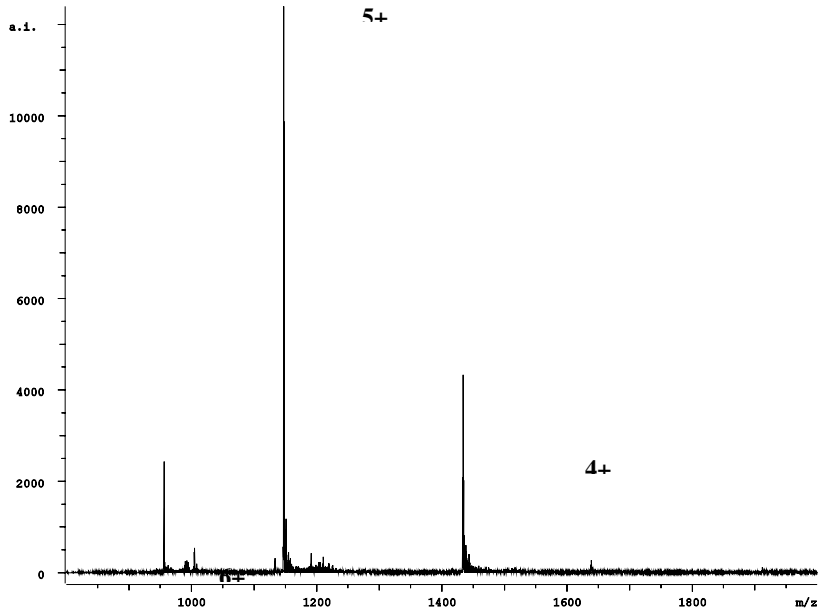

Fig. 12. Electrospray ionisation mass spectrum of bovine insulin obtained using an ion conveyor source.

Fig. 13a shows a mass spectrum detailing the 5+ charge state peak of bovine insulin obtained on the same instrument using an existing commercial (Analytica, Branford, USA) electrospray source. The isotope distribution can be observed with a measured resolution of 7,234 at a signal to noise ratio of 7,263:1. Fig. 13b shows a similar mass spectrum detailing the 5+ charge state peak of bovine insulin obtained using the ion conveyor source. In this case the measured resolution of the isotope distribution was 12,480 at a signal to noise ratio of 76,439:1. The improvement in resolution demonstrated by the ion conveyor source may be attributed to lower radial velocity distribution characteristics of the ion packet produced by this new source design and the lower signal to noise ratio indicative of the higher overall beam current available for detection. If the improvement in signal to noise ratio is accounted for solely on the basis of ion counting statistics then the ion current available for detection is 10^2 greater.

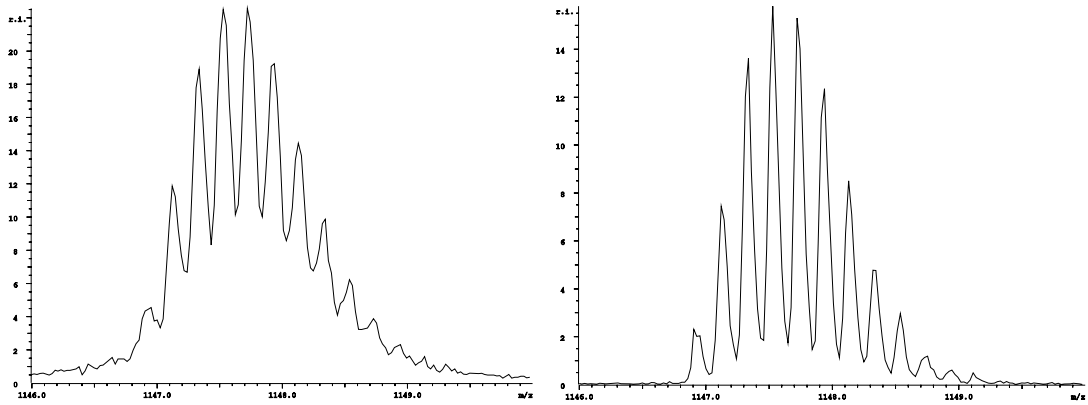

(a) Obtained using a commercial ion source.

(b) Obtained using an ion conveyor source.

Fig. 13. Electrospray ionisation mass spectra of bovine insulin showing the 5+ charge state.

6. Conclusions

A new source design has been developed incorporating new ion conveyor technology and has demonstrated considerably improved performance over a commercially available electrospray ionisation source. Radial focussing and collimation properties of the ion conveyor result in lower radial energy spread in the ion packet produced by the source simultaneously with a two orders of magnitude increase transmission efficiency for detected ions. The new ion conveyor technology has been shown to operate in different modes over a wide pressure range as an efficient ion transmission and ion storage device.

References

[1] M. Yamashita and J. B. Fenn, "Electrospray Ionization Mass Spectrometry Electrospray Ion Source. Another Variation on the Free-Jet Theme", J. Phys. Chem. 88 (1984) 4451.
[2] C. M. Whitehouse, R. N. Dreyer, M. Yamashita and J. B. Fenn, "Electrospray Interface for Liquid Chromatographs and Mass Spectrometers", Anal. Chem. 57 (1985) 675.
[3] M. Mann, C. K. Meng, S. F. Wong, C. M. Whitehouse and J. B. Fenn, "Electrospray Ionization for Mass Spectrometry of Large Biomolecules", Science 246 (1989) 64.
[4] S. M. Hunt, M. M. Sheil, M. Belov and P.J. Derrick, "Probing the Effects of Cone Potential in the Electrospray Ion Source: Consequences for the Determination of Molecular Weight Distributions of Synthetic Polymers", Anal. Chem., 70 (1998) 1812.
[5] R. B. Cole, "Electrospray Ionisation Mass Spectrometry: Fundamentals, Instrumentation & Applications", Wiley, New York (1997).
[6] Y. Zhang, "Development of Electrospray Ionization of Biomolecules on a Magnetic Sector Mass Spectrometer", Ph.D. thesis, University of Warwick, UK (2002).
[7] D. Gerlich, "Inhomogeneous Fields: A Versatile Tool for the Study of Processes with Slow Ions", Advances in Chemical Physics Series, Vol. LXXXII (1992).
[8] E. A. Dynin and N. J. Kirchner, "Ion Processing: Towards a Massively Parallel Mass Spectrometer", 43rd ASMS Conference on Mass Spectrometry and Allied Topics, Atlanta, Georgia (1995).
[9] S. A. Shaffer, K. Tang, G. A. Anderson, D. C. Prior, H. R. Udseth and R. D. Smith, "A Novel Ion Funnel for Focusing Ions at Elevated Pressure Using Electrospray Ionization Mass Spectrometry", Rapid Commun. Mass Spectrom. 11 (1997) 1813.
[10] S. A. Shaffer, D. C. Prior, G. A. Anderson, H. R. Udseth and R. D. Smith, "An Ion Funnel Interface for Improved Ion Focusing and Sensitivity Using Electrospray Ionization Mass Spectrometry", Anal. Chem. 70 (1998) 4111.
[11] W. Paul and H Steinwedel, "A new mass spectrometer without magnetic field", Z. Naturforch., 8a (1953) 448-450.
[12] T. Kim, A. V. Tolmachev, R. Harkewicz, D. C. Prior, G. A. Anderson, H. R. Udseth and R. D. Smith, "Design and Implementation of a New Electrodynamic Ion Funnel", Anal. Chem. 72 (2000) 2247.
[13] M. E. Belov, M. V. Gorshkov H. R. Udseth, G. A. Anderson and R. D. Smith, "Zeptomole-Sensitivity Electrospray Ionisation – Fourier Transform Ion Cyclotron Resonance Mass Spectrometry of Proteins", Anal. Chem. 72 (2000) 2271.
[14] A. W. Colburn, A. E. Giannakopulos and P. J. Derrick, "The Ion Conveyor. An Ion Focusing and Conveying Device", Eur. J. Mass Spectrom. 10 (2004) 149
[15] D. A. Dahl, "SIMION 3D Version 7.0", Proceedings of the 43rd ASMS Conference on Mass Spectrometry and Allied Topics, Atlanta, Georgia (1995) 717.
[16] M. E. Belov, A. W. Colburn and P. J. Derrick, "Design and performance of an electrospray ion source for magnetic-sector mass spectrometers", Rev. Sci. Instum., 69 (1997) 1275.